

icance is not clear; however, the fact that the pseudoscalar line and ω^0 line are parallel is important in that it allows one to predict the momentum-transfer dependence of other processes that proceed through the Feynman diagram shown in Fig. 1(a).

If two mesons are emitted at the upper vertex, the resulting missing-mass spectra will not be the normal two-body phase space, but the phase space multiplied by the factors just obtained [$Q^{-14,8}$ or $Q^{-10,8} \times (t - m_p^2)^{-2}$]. This modified phase space obviously fits the data better than the regular phase space (Fig. 3). When a $\pi\pi$ scattering length is included, the best fits are for $\alpha_0 = 0.28m_\pi^{-1}$ and $0.34m_\pi^{-1}$ for the 2- and 3-GeV data, respectively.

The same procedure can be applied to the 750-MeV data (ABC experiment), only here the conditions are somewhat different. In the ABC experiment the He^3 went forward and the meson or mesons backwards in the center-of-mass system. This means that deuteron exchange [Feynman diagram in Fig. 1(b)] produces much lower momentum transfers than proton exchange. The Q^2 now employed is the momentum transfer from the off-mass-shell deuteron to the proton in the He^3 rest system, and the propagator is $(u - m_d^2)^{-1}$. We assume that the same parametrization (momentum-transfer dependence of the cross section) that was found in the 2- and 3-GeV data can be applied to the ABC data since the same $\text{He}^3 \rightleftharpoons d + p$ vertex exists, and hence the same strong Q^2 dependence should occur. The two-body phase space is thus modified, and the result (Fig. 4) is that almost all of the ABC effect or excess is eliminated. It is quite clear that only a small $\pi\pi$ interaction is now required to fit the data, and

again $\alpha_0 \approx 0.3m_\pi^{-1}$ produces the most satisfactory result.

These arguments are not to be taken as a proof that $\alpha_0 = 0.3m_\pi^{-1}$ but rather they show that the enhancements seen in the missing-mass spectrum at the two-pion threshold are caused by the momentum-transfer dependence of the He^3 vertex and that when this is taken into account, the results are compatible with a small scattering length.

I would like to thank R. Van Berg and Eric Groves for assisting with these calculations, and Ralph Amado for his help on this work.

*Work supported in part by the U. S. Atomic Energy Commission.

¹A. Abashian, N. E. Booth, and K. M. Crowe, Phys. Rev. Lett. **5**, 258 (1960).

²H. Brody *et al.*, Phys. Rev. Lett. **24**, 984 (1970).

³N. E. Booth and A. Abashian, Phys. Rev. **132**, 2314 (1963).

⁴E. Groves, Ph.D. thesis, University of Pennsylvania, 1970 (unpublished).

⁵S. Weinberg, Phys. Rev. Lett. **17**, 616 (1966); C. Lovelace, Phys. Lett. **28B**, 264 (1968); H. J. Schnitzer, Phys. Rev. Lett. **24**, 1384 (1970); R. C. Johnson and P. D. B. Collins, Phys. Rev. **185**, 2020 (1969); J. H. Scharenguivel *et al.*, Nucl. Phys. **B22**, 16 (1970); J. C. Botke, Nucl. Phys. **B23**, 253 (1970); I. M. Blair *et al.*, Phys. Lett. **32B**, 528 (1970).

⁶We would like to thank R. Amado for bringing this variable to our attention.

⁷R. Amado, private communication; see also J. D. Stack, Phys. Rev. **164**, 1904 (1967).

⁸B. Maglich *et al.*, Phys. Rev. Lett. **27**, 1479 (1971).

⁹M. Aguilar-Benitez *et al.*, Phys. Rev. Lett. **25**, 1635 (1970).

¹⁰D. Kreinick, private communication.

Study of the Decay $\Lambda(1520) \rightarrow \Sigma(1385)\pi^\dagger$

T. S. Mast, M. Alston-Garnjost, R. O. Bangerter, A. Barbaro-Galtieri, F. T. Solmitz,
and R. D. Tripp

Lawrence Berkeley Laboratory, University of California, Berkeley, California 94720

(Received 8 November 1971)

The decay $\Lambda(1520) \rightarrow \Sigma(1385)\pi$ has been studied in an energy-independent partial-wave analysis of the reaction $K^- p \rightarrow \Lambda\pi^+\pi^-$ in the momentum range 300 to 470 MeV/c. The width is found to be $\Gamma = 1.40 \pm 0.26$ MeV. Combining this result with one recently reported for $\Lambda(1690)$, we obtain a singlet-octet mixing angle $|\theta| = 73^\circ \pm 10^\circ$, in disagreement with the value $\theta = -25^\circ \pm 6^\circ$ derived from the two-body decays of the $J^P = \frac{3}{2}^-$ states.

The decay

$$\Lambda(1520) \rightarrow \Sigma(1385)\pi \quad (1)$$

is forbidden in SU(3) if the $\Lambda(1520)$ is an unmixed

SU(3) singlet. Several experiments have shown evidence for this decay.^{1,2} Mixing between the $\Lambda(1520)$ and the corresponding $\frac{3}{2}^-$ octet member $\Lambda(1690)$ has been used to explain the decay. The

singlet-octet mixing angle can be derived from the rate for Reaction (1) and the rate for

$$\Lambda(1690) \rightarrow \Sigma(1385)\pi. \quad (2)$$

Previous estimates for these decay rates^{1,3} yielded a lower limit for the magnitude of the mixing angle of $21^\circ \pm 5^\circ$.¹ Mixing of this amount was also obtained from the Gell-Mann-Okubo mass relation⁴ and from the two-body decays of these states to $\bar{K}N$ and $\Sigma\pi$.⁵ Thus, the rates for (1) and (2) were considered to be excellent confirmation for the multiplet assignments and the simple hypothesis of singlet-octet mixing.⁵

In this paper we present the results of a detailed analysis of the formation reaction $K^-p \rightarrow \Lambda(1520) \rightarrow \Lambda\pi^+\pi^-$. We have used an isobar model for the analysis of the three-body final state. The model, as formulated by Deler and Valladas for $\pi N \rightarrow \pi\pi N$, has been modified for $\Lambda\pi\pi$ and extended to incorporate knowledge of the Λ polarization coming from its decay.⁶ We obtain a decay rate for (1) of 1.40 ± 0.26 MeV, which is more than twice as large as the previous measurement¹ of 0.67 ± 0.17 MeV. In addition, in making SU(3) comparisons, our calculation of the phase-space ratio between Reactions (1) and (2) disagrees by a factor of 3 with that of Ref. 1. Finally, a recent isobar analysis⁷ of Reaction (2) has yielded a decay rate an order of magnitude lower than the previous upper limit.³ Using these new values there is an overall disagreement by about a factor of 70 with the description of Reactions (1) and (2) based upon mixing between the generally accepted $\frac{1}{2}^+$ singlet and octet states.

An exposure of 11 events/ μb in the Berkeley 25-in. hydrogen bubble chamber has yielded about 9000 events of the type $K^-p \rightarrow \Lambda\pi^+\pi^-$ with K^- momenta between 300 and 470 MeV/c.⁸ We first present a semiquantitative discussion of the

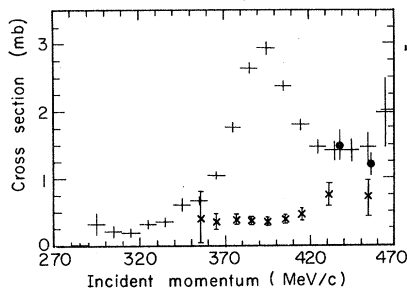


FIG. 1. Cross section for $K^-p \rightarrow \Lambda\pi^+\pi^-$ as a function of incident K^- momentum. The crosses represent the background to the $\Lambda(1520)$ resonance, obtained through the partial-wave analysis discussed in the text. The dots are from the work of Armenteros (Ref. 9).

structure in the data.

The momentum dependence of the partial cross section (Fig. 1) is dominated by the $\Lambda(1520)$ near 400 MeV/c, but a substantial nonresonant background exists beyond the resonance. A visual interpolation of the background to 395 MeV/c would suggest that 80–90% of the cross section at resonance comes from the resonance itself. (The background shown as crosses results from the analysis discussed later.) The question then arises of how much of this resonance contribution proceeds through the quasi-two-body Reaction (1). Information about this is given in the Dalitz plot, mass distributions, and the production and decay angular distributions.

The Dalitz plot at the resonant energy (390–400 MeV/c) and its projections are shown in Fig. 2. Enhancements at the high $\Lambda\pi$ invariant masses indicate the presence of $\Sigma(1385)$ (actually centered outside the kinematically allowed region). There is increased density at low $\pi\pi$ mass, indicating constructive interference between $\Sigma^-(1385)$ and $\Sigma^+(1385)$ and hence dominance of symmetric $I=0$ production. Further information on the isospin composition is given from a separate analysis of the $\Lambda\pi^0\pi^0$ channel from the same exposure. At all momenta the $\Lambda\pi^0\pi^0$ cross section is approximately half that of $\Lambda\pi^+\pi^-$, as expected for pure $I=0$ production. A more sensitive measure of the

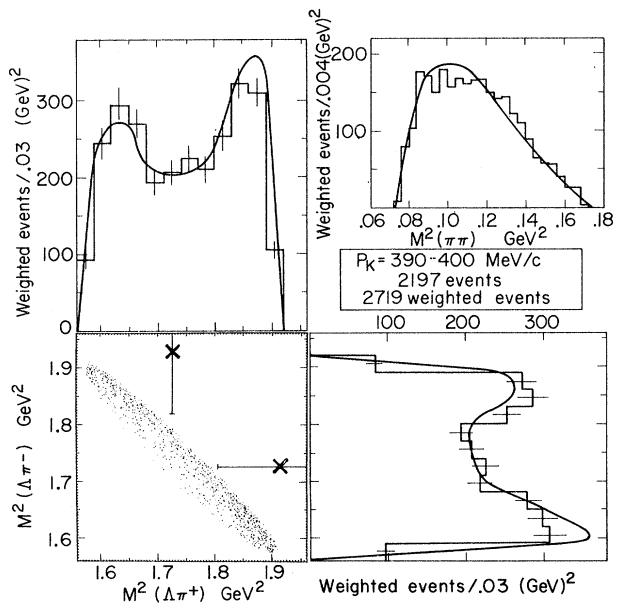


FIG. 2. Dalitz plot and projections for events in the momentum interval 390–400 MeV/c. The curves result from the partial-wave analysis discussed in the text. The symbols (crosses) in the lower left-hand plot indicate the $\Sigma(1385)$ bands.

presence of $I=1$ contributions comes from the charge asymmetry of the Dalitz plot, $(N^- - N^+) / (N^- + N^+)$, where N^- is the number of events with a $\Lambda\pi^-$ mass larger than a $\Lambda\pi^+$ mass. This asymmetry, shown as a function of incident momentum in Fig. 3(d), arises from a difference between the $\Sigma^-(1385)$ and $\Sigma^+(1385)$ masses¹⁰ and from $I=0$ and $I=1$ interference. An $I=1$ amplitude about 10% as large as the resonant $I=0$ amplitude is sufficient to explain the observed structure. Thus the $I=1$ contribution to the partial cross section is of the order of a few percent.

Figures 3(a)–3(c) show the Legendre polynomial coefficients for the Λ angular distribution and polarization as a function of incident K^- momentum. Here the large A_2/A_0 coefficient with a maximum in the vicinity of the resonance is consistent with the Reaction (1) interpretation. However, the large structure in A_1/A_0 and the appreciable B_1/A_0 polarization coefficient shows that even-parity states are also present in significant amounts. The dots are from the partial-wave analysis discussed next.⁸

We now describe the results of the complete analysis of the $\Lambda\pi^+\pi^-$ reaction by means of an isobar model. The data between 350 and 470 MeV/c were divided into nine bins in incident K^- momentum. The data in each bin were fitted independently by a maximum-likelihood fit using up to seventeen partial waves chosen to describe the data. These include S , $P1$, $P3$, and $D3$ partial waves for the incoming state (in two isospin states) and four types of isobars: (a) “ Y^* ,” a $\Lambda\pi$ system resonating as $\Sigma(1385)$; (b) “ $\Lambda\pi$,” a $\Lambda\pi$

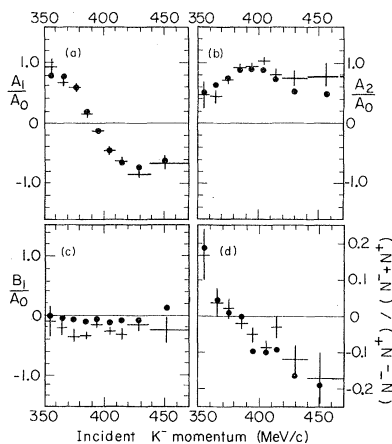


FIG. 3. Legendre polynomial coefficients for the Λ angular distribution (a), (b) and polarization (c), and charge asymmetry of the Dalitz plot (d), as a function of incident momentum. The dots are results from the partial-wave analyses.

system in a relative S wave; (c) “ σ ,” an S -wave $\pi\pi$ system; and (d) “ ρ ,” a P -wave $\pi\pi$ system.¹⁰ Many of these amplitudes were found to be zero within errors for most of the momentum intervals and so were discarded. In this manner, by successive elimination and remaximization, satisfactory solutions at all nine momenta were found using only six of the amplitudes. Argand plots of these six amplitudes are shown in Fig. 4. Here we have chosen the arbitrary phase inherent in a reaction process to be fixed by the dominant $Y^* DS03$ resonant Breit-Wigner form.¹¹ The energy dependence of this form will be discussed later.

The amplitudes imply that Reaction (1) described by the $Y^* DS03$ amplitude dominates the cross section at resonance. The S -wave di-pion in the $DP03$ state is also fed by the $\Lambda(1520)$ resonance, but to a much smaller degree. The other amplitudes which are fed by nonresonant incident states give magnitudes which are plausible from angular-momentum barrier considerations. The small $Y^* DS13$ amplitude along with the $\Sigma^+(1385)$ - $\Sigma^-(1385)$ mass difference is sufficient to explain the asymmetry in the Dalitz plot [Fig. 3(d)].

The overall magnitude of the waves is fixed to agree with the measured partial cross section (Fig. 1). The relative amounts of each wave, however, have been freely chosen by the fit. Thus, it is of interest to compare the magnitude

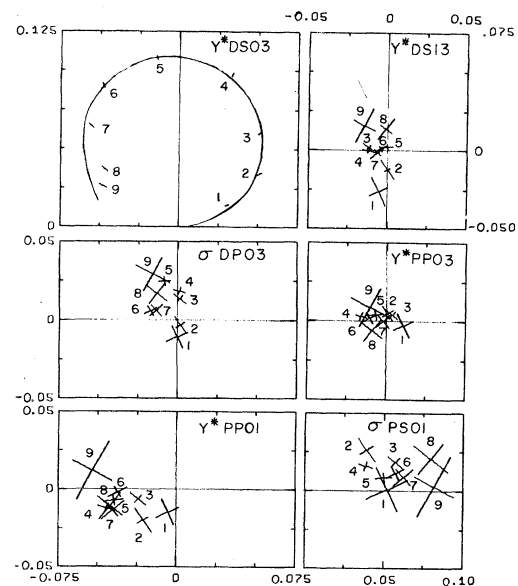


FIG. 4. Partial-wave amplitudes with statistical errors resulting from the fits discussed in the text. The numbers 1 through 9 indicate successive incident K^- momentum intervals (same as in Fig. 3). The curve on the $Y^* DS03$ partial wave is explained in the text.

of the $Y^* DS03$ with that expected for a Breit-Wigner resonance with appropriate centrifugal barriers for all channels fed by the resonance: D -wave barriers ($r=1$ F) for the $\bar{K}N$ and $\Sigma\pi$ partial widths; S wave for decay mode (1). The phase space for (1), given by the effective relative momentum of the $\Sigma(1385)$, was determined by averaging the momentum over the P -wave Breit-Wigner shape with a width of 40 MeV. The curve in Fig. 4 corresponds to the resulting Breit-Wigner form, and the good agreement with the energy-independent points confirms the momentum dependence of the form.

The total $\Lambda\pi\pi$ cross section at the resonant energy contains 0.40 mb from nonresonant background and 2.53 mb from the $\Lambda(1520)$ (1.96 mb from $Y^* DS03$, 0.11 mb from $\sigma DP03$, and 0.46 mb from the interference of these two waves). This resonance cross section yields 0.11 ± 0.01 for the branching fraction of the $\Lambda(1520)$ into $\Lambda\pi\pi$, in agreement with the world average.¹²

Defining a branching fraction $R = [\Lambda(1520) \rightarrow \Sigma(1385)\pi] / [\Lambda(1520) - \text{all } \Lambda\pi\pi]$, each of the five momentum intervals centered on the $\Lambda(1520)$ resonance (intervals 3-7) yields a value ~ 0.8 . The overall value is $R = 0.82 \pm 0.10$, where the error is estimated by altering some of the input parameters of the model¹⁰ and by studying the sensitivity of R to the inclusion of different sets of amplitudes consistent with a reasonable energy continuity. This result is in strong disagreement with the value $R = 0.39 \pm 0.10$ quoted from the production experiment.¹² Using the world average values¹³ for the $\Lambda(1520)$ total width and branching fraction into $\Lambda\pi\pi$, we obtain $\Gamma = 1.40 \pm 0.26$ MeV for Reaction (1).

We wish to compare this partial width at resonance for Reaction (1) with that for Reaction (2). An upper limit for the width for Reaction (2) was obtained from a reported enhancement in the $\Lambda\pi^+\pi^-$ cross section.³ However, a more recent experiment with increased statistics found no structure in the $\Lambda(1690)$ region. An isobar model fit to the recent data found an amplitude at resonance of -0.06 ± 0.03 (Ref. 7 and Barloutaud¹⁴) which yields a partial width of $1.0^{+2.4}_{-0.9}$ MeV.

The mixing angle between the singlet and octet members is related to the coupling constants for decays (1) and (2) by $\tan\theta = G_{1520}/G_{1690}$. The measured partial widths are related to the coupling constants by $\Gamma = G^2 \int |M(Y^* DS03)|^2 d\rho$, where $M(Y^* DS03)$ is the matrix element for the decay, given by the isobar model^{6,8}, and the integral is over the three-body phase space. The ratio of

this integral at 1520 and 1690 MeV is 9.5 .¹⁵ Using this ratio, our measurement of the decay rate, and a mixing angle of 25° , we would predict the partial width for Reaction (2) to be some 60 MeV, rather than the measured value of 1 MeV. Thus the interpretation of simple singlet-octet mixing is now in gross disagreement with the observed rates for (1) and (2). Alternatively, we can calculate $|\theta|$ from the observed rates. In this case $|\theta| = 73^\circ \pm 10^\circ$ instead of $25^\circ \pm 6^\circ$. A possible explanation of this discrepancy may involve mixing of these states with another octet as predicted by the quark model.¹⁶

Note added in proof.—The work of Chan *et al.*² has now been published [Phys. Rev. Lett. **28**, 256 (1972)]. Their analysis also finds that the $\Lambda\pi\pi$ final state of the $\Lambda(1520)$ is dominated by $\Sigma(1385)\pi$. However, the amount of $\Lambda\pi\pi$ cross section they attribute to $\Lambda(1520)$ is in strong disagreement with the results of our analysis.

†Work done under the auspices of the U. S. Atomic Energy Commission.

¹E. Burkhardt *et al.*, Nucl. Phys. **B27**, 64 (1971).

²S.-b. Chan *et al.*, *Hyperon Resonances-70*, edited by F. C. Fowler (Moore Publishing Co., Durham, North Carolina, 1970), p. 79. Also D. Cline *et al.*, presented to the Fourteenth International Conference on High Energy Physics, Vienna, Austria, September 1968 (unpublished), paper No. 922.

³J. H. Bartley *et al.*, Phys. Rev. Lett. **21**, 111 (1968).

⁴In addition to the $\Lambda(1690)$, other members of the $\frac{3}{2}^-$ octet are assumed to be $N(1520)$, $\Sigma(1670)$, and $\Xi(1815)$.

⁵R. Levi-Setti, in *Proceedings of the Lund International Conference on Elementary Particles*, edited by G. von Dardel (Berlingskas Boktryckeriet, Lund, Sweden, 1970), p. 339. The mixing angle was recently recalculated to be $\theta = -25^\circ + 6^\circ$ by D. E. Plane *et al.*, Nucl. Phys. **B22**, 93 (1970).

⁶B. Deler and G. Valladas, Nuovo Cimento **45A**, 559 (1966); D. Morgan and G. Shaw, Phys. Rev. D **2**, 520 (1970).

⁷J. Prevost *et al.*, in Proceedings of the Amsterdam International Conference on Elementary Particles, 30 June-6 July 1971 (to be published).

⁸Details about the data as well as the analysis will be presented in a longer paper. See T. S. Mast, Lawrence Berkeley Laboratory Report No. LBL 301, 1971 (unpublished).

⁹R. Armenteros *et al.*, Nucl. Phys. **B21**, 15 (1970).

¹⁰For the $\Sigma(1385)$ we have used $M^+ = 1384$ MeV, $M^- = 1388$ MeV, and $\Gamma = 40$ MeV. For the S -wave $\Lambda\pi$ system we have used the parameters obtained by B. R. Martin and M. Sakitt, Phys. Rev. **183**, 1352 (1969). The parametrization of the $\pi\pi$ phase shifts for " σ " and " ρ " waves have been taken from D. Morgan, Phys. Rev. **166**, 1731 (1968).

¹¹The notation here is $LL'I2J$, where L and L' refer to the orbital angular momentum for the incoming K^-p system and the outgoing quasi-two-body system (Y^* or σ), respectively, I is the isotopic spin of the $\Lambda\pi^+\pi^-$ system, and J is the total angular momentum of the $\Lambda\pi^+\pi^-$ system. For L' only S and P waves were used.

¹²The experiment of Ref. 1 has many fewer events (206 events) than the present experiment and has the additional problem of extracting the $\Lambda(1520)$ signal from the $\Lambda\pi^+\pi^-\pi^0$ final states. The data were divided into three mass intervals centered on the $\Lambda(1520)$. The data in the central interval (with about 15% background) agree with ours and yield a branching fraction consistent with ours. The data in the side intervals (with about 30% background) yield lower branching fractions and contribute to their low overall value.

¹³A. Rittenberg *et al.* (Particle Data Group), Rev. Mod.

Phys. Suppl. 43, 1 (1971). $\Gamma(1520) = 16 \pm 2$ MeV; the branching fraction of $\Gamma(1520)$ into $\Lambda\pi\pi$ is $(9.6 \pm 0.6)\%$; the branching fraction of $\Sigma(1385)$ into $\Lambda\pi$ is $(90 \pm 3)\%$.

¹⁴The estimate of the range of uncertainty on the amplitude is from R. Barloutaud, private communication.

¹⁵The formula used in Ref. 1 [Eq. (12)] to calculate an effective integral of the matrix element squared, by calculating an average $\Sigma(1385)$ momentum, uses an incorrect normalization for the $\Sigma(1385)$ Breit-Wigner term. The normalization should not depend on the particular kinematic region being weighted. Note that independent of this correction there is still a disagreement by a factor of 20 with the previous SU(3) fits.

¹⁶See, for example, R. H. Dalitz, in *Symmetries and Quark Models*, edited by R. Chand (Gordon and Breach, New York, 1970); also, D. Faiman and A. W. Hendry, Phys. Rev. 173, 1720 (1968).